ADVANCED ENERGY MATERIALS
www.advenergymat.de

Tailored TiO_2 Protection Layer Enabled Efficient and Stable Microdome Structured p-GaAs Photoelectrochemical Cathodes

Shiyao Cao, Zhuo Kang, Yanhao Yu, Junli Du, Lazarus German, Jun Li, Xiaoqin Yan, Xudong Wang,* and Yue Zhang**

Group III–V compound semiconductors are a promising group of materials for photoelectrochemical (PEC) applications. In this work, a metal assisted wet etching approach is adapted to acquiring a large-area patterned microdome structure on p-GaAs surface. In addition, atomic layer deposition is used to deposit a TiO_2 protection layer with controlled thickness and crystallinity. Based on a PEC photocathode design, the optimal configuration achieves a photocurrent of –5 mA cm^{-2} under –0.8 V versus Ag/AgCl in a neutral pH electrolyte. The TiO_2 coating with a particular degree of crystallization deposited via controlled temperature demonstrates a superior stability over amorphous coating, enabling a remarkably stable operation, for as long as 60 h. The enhanced charge separation induced by favorable band alignment between GaAs and TiO_2 contributes simultaneously to the elevated solar conversion efficiency. This approach provides a promising solution to further development of group III–V compounds and other photoelectrodes with high efficiency and excellent durability for solar fuel generation.

1. Introduction

The ideal band gap and excellent photophysical properties positioned III–V compounds as promising photoelectrode candidates in a photoelectrochemical (PEC) system.[1] Among these materials, GaAs has a remarkable electron mobility of 9200 cm^2 V^{-1} s^{-1} and a hole mobility up to 400 cm^2 V^{-1} s^{-1}, which are desired for obtaining high PEC performance.[2] Their practical applications, however, are largely limited by their active chemistry and strong tendency to be corroded in PEC electrolytes. According to the Pourbaix diagrams, III–V compounds all have an very narrow window of stability.[3] It has been proven that GaAs can be stable in acidic solutions under open circuit voltage (OCV) or cathodic conditions for a long time.[4] However, when used as a photoanode, GaAs can dissolve quickly in alkaline environments. Severe photocorrosion results in continues dissolution of GaAs. Protection layers peels off during the reaction making GaAs difficult to protect.[5] In near neutral solution GaAs photoanode and photocathode would both typically fail within 30 min.[6] Practically, PEC devices need to have efficiencies of at least 10% with a lifetime longer than 10 years (≈30 000 on-sun hours, i.e., ≈90 000 total operating hours) in order to be cost effective.[7] In order to bring the promising physical properties of GaAs to PEC applications, many efforts have been investigated to stabilize the material. Predominate strategy is to introduce protection films to the GaAs surfaces, such as epitaxial metal oxide layers, optically thick metals, and covalent attachments. These approaches have successfully extended the lifetime of GaAs photoelectrodes.[8]

Recently, atomic layer deposition (ALD) has been broadly used for surface protection in many electrochemical systems.[9,10] Its conformal and pinhole-free feature allows the protection film to be made very uniform and ultrathin over rough or irregular surfaces. It has been shown that a few nanometer-thick TiO_2 thin film could effectively protect nanostructured black-Si surface[11] and extend the lifetime of planar Si photoanode to more than 600 h in 1 M NaOH aqueous solution electrolyte.[12] Inspired by these discoveries, here we report an application of ALD TiO_2 protection layer on microstructured p-GaAs photocathode for PEC water splitting. A metal assisted wet etching process was used to create a large-area patterned microdome array on p-GaAs surface. The optimized TiO_2 layer was able to offer superior protection, yielding a remarkable stability as long

S. Y. Cao, Prof. Z. Kang, J. L. Du, Prof. X. Q. Yan, Prof. Y. Zhang
Beijing Advanced Innovation Center for Materials Genome Engineering
State Key Laboratory for Advanced Metals and Materials
School of Materials Science and Engineering
University of Science and Technology Beijing
Beijing 100083, China
E-mail: xqyan@mater.ustb.edu.cn; yuezhang@ustb.edu.cn
Dr. Y. H. Yu, L. German, J. Li, Prof. X. D. Wang
Department of Materials Science and Engineering
University of Wisconsin-Madison
Madison, WI 53706, USA
E-mail: xudong.wang@wisc.edu
Prof. Y. Zhang
The Beijing Municipal Key Laboratory of New Energy Materials and Technologies
University of Science and Technology Beijing
Beijing 100083, China
The ORCID identification number(s) for the author(s) of this article can be found under https://doi.org/10.1002/aenm.201902985.

DOI: 10.1002/aenm.201902985

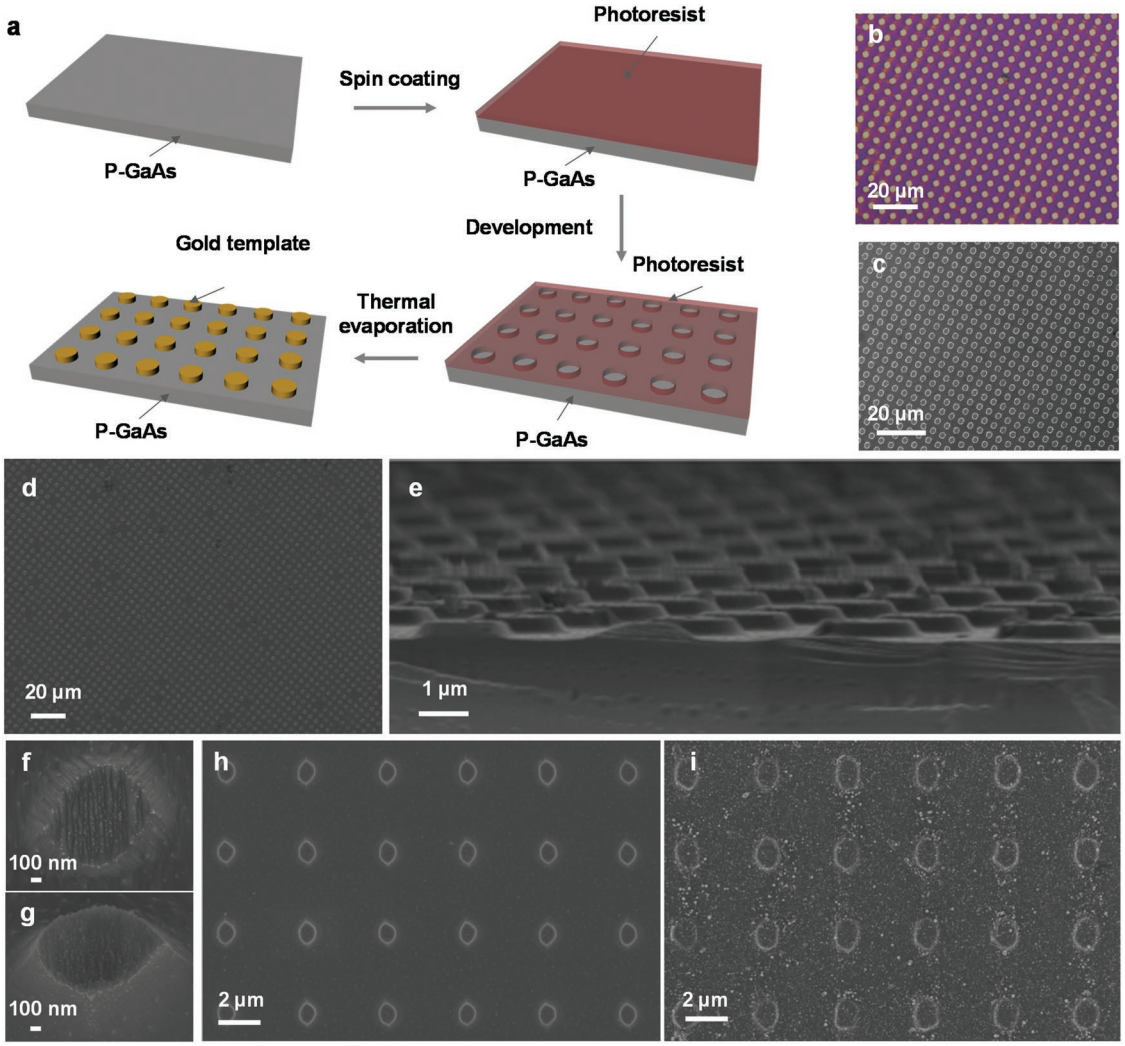

Figure 1. Fabrication process and SEM characterization of patterned p-GaAs photocathode surface. a) Schematic synthesis processes of p-GaAs microdome arrays using Au-assisted lithography. b) Optical microscope image of the p-GaAs surface with a patterned positive photoresist film. c) SEM image of the p-GaAs surface with a patterned Au template. d) A large-area image of as-processed microdome pattern on the p-GaAs wafer. e) A cross-sectional image of the p-GaAs microdome arrays. f) Enlarged image showing the surface structure of one microdome. g) A 45°-titled view of a microdome structure. h) 26 nm TiO_2 coated p-GaAs microdome surface. i) TiO_2-coated p-GaAs microdome surface with Pt nanoparticles.

as 60 h at a photocurrent of –5 mA cm^{-2} in neutral pH electrolyte. Our work presents a promising path to bringing III–V compounds to efficient and stable PEC devices.

2. Results and Discussion

Microdome patterns were created on planar (100)-oriented p-GaAs wafer surface by metal-assisted chemical etching using 2 μm mesh patterns (see the Experimental Section and **Figure 1**a for details). Au pattern was deposited through the mesh and used to direct the etching in a $KMnO_4/H_2SO_4$ solution. The optical microscope image of a p-GaAs with a thin patterned photoresist mask on the surface is shown in Figure 1b. After the thermal evaporation of Au on the wafer with patterned mask and lift-off process, the wafer with patterned Au template was successfully fabricated. Figure 1c shows the SEM image of p-GaAs with patterned Au template. As shown by the scanning electron microscopy (SEM) image in Figure 1d, the as-processed GaAs surface had a uniformly array of circular dots over the entire wafer surface (larger area optical image is shown in Figure S1 in the Supporting Information). The size and spacing of the pattern perfectly matched to the mesh mask, showing excellent etching confinement of Au metal. A small amount of missing spots could also be observed, possibly because some Au templates fell off during the etching process. All the microdomes had a uniform height of ≈350 nm, as shown in the cross-sectional image (Figure 1e). An enlarged SEM image in Figure 1f revealed that the circular feature had a dome-shape. The top surface of the dome had a size of 1.6 μm in diameter, while the dome base was 1.9 μm wide. This size variation indicates side etching happened during the etching process.[13] Small roughness could also be observed from the dome surface, which was a result

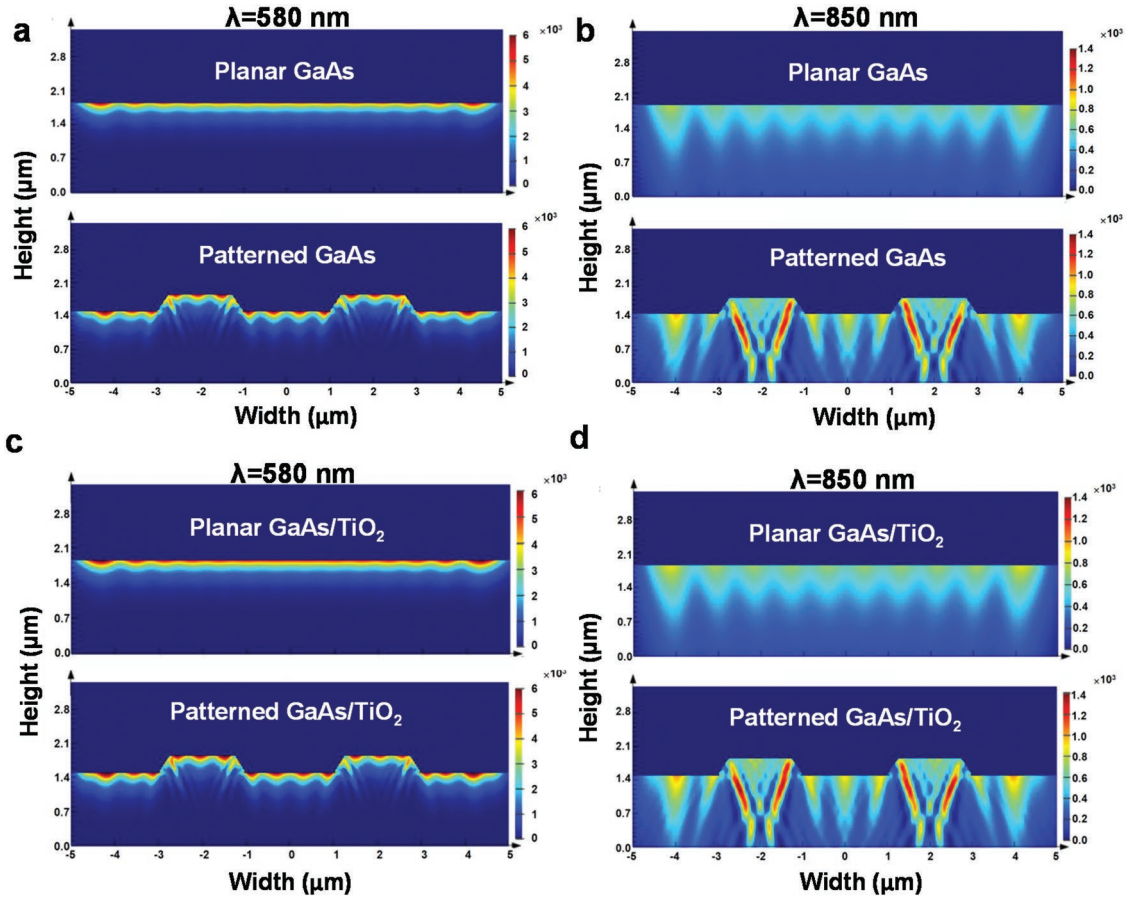

Figure 2. Optical studies of microdome structured p-GaAs photocathode. a,b) FDTD simulated optical absorption profiles in planar and microdome structured p-GaAs under the illumination of monochromatic lights with a wavelength of a) 580 nm and b) 850 nm. c,d) FDTD simulated optical absorption profiles in planar and microdome structured p-GaAs/TiO_2 under the illumination of monochromatic lights with a wavelength of c) 580 nm and d) 850 nm.

of the uneven thickness of the deposited gold template. A 45°-titled view of the microdome further revealed the smooth size variation along the height direction, and the small surface features were nanometer-scale surface bumps (Figure 1g). All the microdome structures were well preserved after 26 nm TiO_2 ALD deposition (Figure 1h). No distinguishable surface feature other than the circular dome top can be observed after TiO_2 deposition, which confirmed the uniform and high-quality TiO_2 film coverage. After Pt deposition, uniformly distributed Pt nanoparticles can be clearly seen from the TiO_2-coated GaAs surface (Figure 1i). The presence of rich Pt was further confirmed by energy dispersive spectrometer (EDS) (Figure S2, Supporting Information).

The light absorption behavior of the microdome patterned p-GaAs was first studied using 2D finite-difference-time-domain (FDTD) simulations and compared to planar surfaces (simulation details are included in Figure S3 in the Supporting Information). As shown in **Figure 2**a, under visible light illumination (wavelength of 580 nm), the planar surface showed a fairly uniform electric field intensity at the center flat region; whereas enhanced intensity was observed at the edges of the flat surface. This enhancement can be attributed to the light-trapping effect along the edges, which leads to enhanced internal light scattering and thus higher light absorption.[12] Such an enhanced absorption became more significant when periodic microdomes were introduced to the surface, as the gaps of microdomes and the edges of dome-tip drastically increased the interactions among the incident lights. When the incident wavelength increases, this interaction is further intensified. As shown in Figure 2b, for an incident light with a wavelength of 850 nm, the microdome feature could induce a strong penetration of wave intensity up to >2 μm deep inside the GaAs wafer. FDTD simulations further showed that the 26 nm TiO_2 protection layer had negligible influence to the light absorption behavior (Figure 2c,d).

To confirm the light absorption merits of the microdome arrays, UV–vis reflection was measured and compared (Figure S4, Supporting Information). Both microstructured and planar GaAs wafers showed an absorption edge at 880 nm, corresponding to the band gap of 1.4 eV. The p-GaAs wafer with microdome arrays showed a universal (≈15%) lower reflection across the entire visible wavelength range (400–900 nm), compared to the planar p-GaAs wafer. This UV–vis reflection result is consistent with the FDTD simulation, and confirmed the patterned microdome feature was able to enhance light absorption and potentially improve the PEC performance.

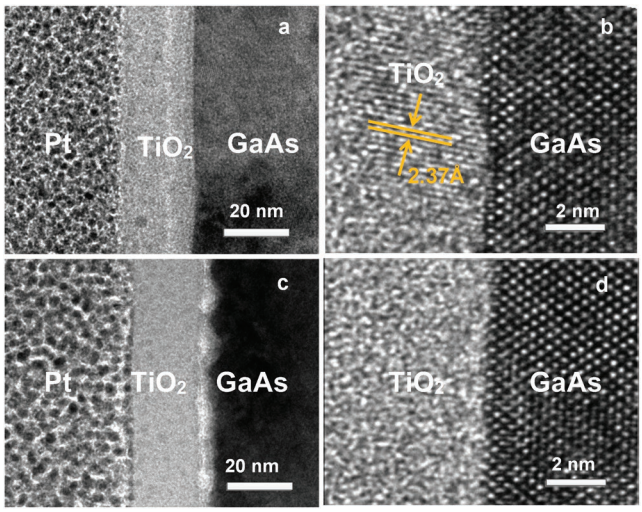

Figure 3. TEM image of TiO_2 films deposited with a) 300 cycles under 300 °C, c) 300 cycles under 150 °C. High resolution TEM image of TiO_2 films deposited with b) 300 cycles under 300 °C and d) 300 cycles under 150 °C of atomic layer deposition on GaAs.

In order to improve the PEC stability, TiO_2 protection layers were introduced to the GaAs surface by ALD with different film parameters. The band alignment between p-GaAs and n-type TiO_2 has a typical type II alignment. Therefore, upon illumination, photoexcited electrons can drift from p-GaAs to n-TiO_2 and then inject into the electrolyte with a large driving force. The much lower valence band of TiO_2 is favorable for blocking holes from entering the cathode interface, and thus improves the charge exchange efficiency.

TEM samples were prepared by the focused ion beam (FIB) (see the Experimental Section and Figure S5a,b in the Supporting Information for details). The protection performance of ALD TiO_2 coating was first investigated on planar GaAs photocathodes. TiO_2 films were deposited at two different temperatures of 150 and 300 °C. At each temperature, two different ALD cycle numbers (50 and 300) were used. TiO_2 thin film grown at 300 °C for 300 cycles (referred as 300 C) had a uniform thickness of 26 nm (**Figure 3**a and Figure S6a, Supporting Information) giving the growth rate of ≈0.087 nm per cycle. High resolution transmission electron microscopy (HRTEM) image revealed the structure of the TiO_2 film grown under 300 °C for 300 cycles. The small crystal particles dispersed in the film were identified to be the anatase phase (Figure 3b). TiO_2 thin film grown at 150 °C for 300 cycles (referred as 300 A) showed a thickness of 20 nm (Figure 3c and Figure S6b, Supporting Information) giving a growth rate of 0.067 nm per cycle. No crystal lattice fringe could be observed from the HRTEM image, confirming the amorphous phase of the 150 °C TiO_2 film (Figure 3d). 50 cycles of ALD TiO_2 (referred as 50 A and 50 C, respectively) exhibited the same growth rate for each temperature, which yielded a thickness of 3 nm at 150 °C and 4 nm at 300 °C, respectively.

Schematic of the electronic structure of the photocathode under illumination was illustrated in **Figure 4**a. As shown in Figure 4b, all the TiO_2-coated planar GaAs photocathodes decorated with Pt exhibited a higher saturated J_{ph} comparing to the pristine GaAs–Pt. This general PEC enhancement due to TiO_2 coating could be attributed to the passivation of surface defect states, which suppressed surface recombination and improved water reduction efficiency.[14] All the J_{ph}–V curves exhibited a two-stage hydrogen evolution feature, where one small intermediate H^+ ion reduction peak appeared at ≈–0.8 to 0.9 V versus Ag/AgCl and J_{ph} reached saturation at –1.3 V versus Ag/AgCl. For the 150 °C amorphous coating, the 3 nm TiO_2-coated GaAs (50 A) exhibited a saturated J_{ph} of –9.21 mA cm^{-2}. When the TiO_2 thickness increased to 20 nm (300 A), the saturated J_{ph} dropped to –7.25 mA cm^{-2}. This was because thicker TiO_2 film had higher resistance for electrons to tunnel through, especially for the passage of a high current density (>1 A cm^{-2}).[9,15] In addition, the intermediate H^+ ion reduction peak shifted from –0.85 to –0.8 V, as the TiO_2 thickness increased from 3 to 20 nm. This was possibly due to the adsorption difference of H^+ ions at GaAs/TiO_2/Pt electrode surface.[16] The 300 °C coating led to an even higher PEC performance. 4 nm TiO_2 protection layer (50 C) yielded a saturated J_{ph} of –10.55 mA cm^{-2}. This value decreased to –9.15 mA cm^{-2} as the coating thickness increased to 26 nm (300 C). In addition, the 4 nm TiO_2-coated photocathode (50 C) exhibit the same H^+ ion reduction peak at –0.8 V; whereas the thicker TiO_2 coating (300 C) shifted the peak to –0.76 V, suggesting the TiO_2 grown under 300 °C thin film (300 C) surface had less significant influences to H^+ absorption.[17]

PEC performance was then characterized from the microdome structured p-GaAs (with Pt nanoparticle decoration) under one sun illumination (AM 1.5G) in 0.1 M potassium phosphate electrolyte solution (pH 7) from an exposed photoactive area of ≈0.1 cm^2. Figure 4c shows the J_{ph}–V curves in comparison to planar GaAs. Both electrodes exhibited the same curve features, suggesting the electrochemical property of p-GaAs was not changed by the formation of microdomes. The small H^+ reduction peak appeared at ≈–0.9 V versus Ag/AgCl from both curves. The planar p-GaAs–Pt electrode exhibited a saturated J_{ph} of –7.15 mA cm^{-2}. The p-GaAs with microdome structures reached a much higher saturated J_{ph} of –9.45 mA cm^{-2} as a result of enhanced light absorption and enlarged surface area. As the microdome structured GaAs surface was protected by 26 nm TiO_2 deposited under 300 °C, the PEC performance was further improved with a saturated J_{ph} reaching about –12.06 mA cm^{-2}. Same as the planar GaAs photocathodes, this enhancement could be attributed to the removing of surface defects or dangling bonds by ALD coating. Electrochemical impedance spectroscopy (EIS) of the TiO_2 coated and uncoated GaAs further evidenced the charge transfer enhancement. As shown in Figure S7 (Supporting Information), all the Nyquist plots contain a semicircle portion at high frequencies, suggesting an electron transfer limited process. From the plot, the 26 nm TiO_2 deposited under 300 °C coated sample showed a significantly smaller semicircle, which was corresponding to a lower charge transfer resistance and a higher charge separation efficiency.

The stability test was then performed on all GaAs-based photocathodes. As expected, neither of the unprotected photocathodes (planar and microdome structured GaAs) could maintain a stable photocurrent during the potentiostatic test at –0.8 V versus Ag/AgCl (Figure S8, Supporting Information). The J_{ph} of both photocathodes dropped rapidly by more than 90% within half an hour. Same as others' reports,[5,6,9,18] the GaAs surface

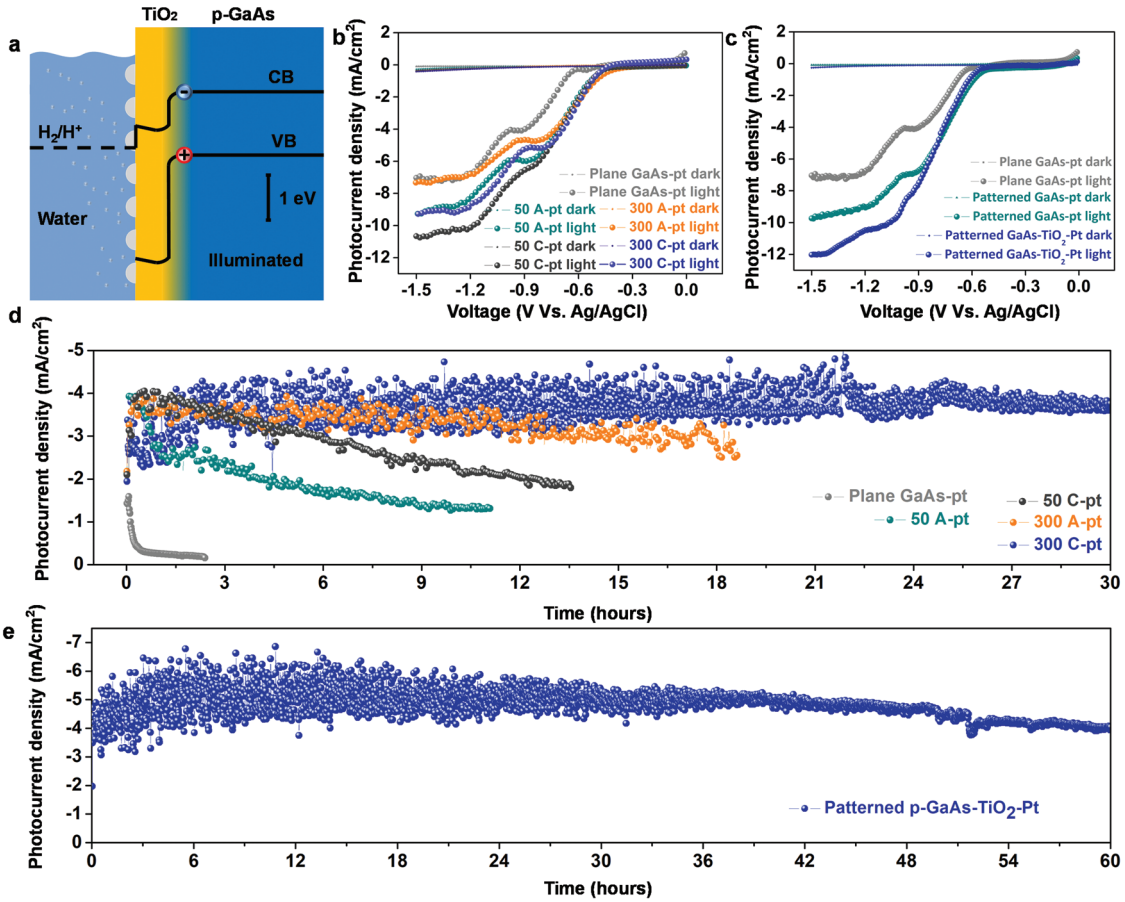

Figure 4. PEC performance of GaAs-based photocathodes. a) Schematic band structure of the TiO_2/p-GaAs photocathode at 0 V RHE under illumination. CB and VB denote the conduction and valence bands, respectively. b) J_{ph}–V curves of planar p-GaAs with various ALD TiO_2 protection layers and the decoration of Pt nanoparticles c) J_{ph}–V curves of unprotected planar p-GaAs photocathode with Pt nanoparticles, unprotected patterned p-GaAs photocathode with Pt nanoparticles, and 26 nm TiO_2 layer-protected patterned p-GaAs with Pt nanoparticles. d) Long-term stability performance of planar p-GaAs–Pt without and with various TiO_2 layer protections. e) Long-term stability performance of a 26 nm TiO_2-coated patterned p-GaAs photocathode decorated with Pt nanoparticles.

suffered from serious photocorrosion, oxidized quickly, and lost its catalytic capability (Figure S9a,b, Supporting Information). Significant Pt detachment was also observed due to the corrosion. Compared to the unprotected GaAs photocathodes, all the TiO_2 coated ones exhibited a significantly longer lifetime (Figure 4d). Specifically, both thin amorphous (3 nm) and certain degree of crystallinity thin TiO_2 coatings (4 nm) exhibited a relatively fast performance decay (50 A and 50 C). Started from –4.2 mA cm^{-2}, J_{ph} of the 50 A photocathode dropped 36% in the first 1 h and then continuously dropped to –1.3 mA cm^{-2} in the next 10 h. J_{ph} of 50 C photocathode exhibited an almost linear decay from the initial –4.2 to –1.8 mA cm^{-2} within the first 14 h. Increasing the thickness largely improved the stability. For the 300 A photocathode, J_{ph} slowly decreased from –4.0 to –2.60 mA cm^{-2} during 18 h. The 300 C photocathode had the best performance. Its J_{ph} remained at a nearly constant value of –4 mA cm^{-2} for 30 h of continuous operation with 93% retention of its initial J_{ph} at the 30th hour, confirming an excellent PEC lifetime improvement. SEM further revealed that the protected photocathode had no evidence of corrosion after PEC operation (Figure S9c,d, Supporting Information). The best 300 C protection layer was then applied to the microdome structured p-GaAs photocathodes, which had the highest PEC performance. As shown in Figure 4e, the protected photocathode exhibited a stable J_{ph} for 60 h at –0.8 V versus Ag/AgCl (from the initial –5.08 to –4.07 mA cm^{-2} after 60 h continuous operation). SEM images further revealed that the microdome patterns were intact during the 60 h PEC reaction (Figure S10, Supporting Information). A large oscillation of the J_{ph} was also observed at the first 20 h of PEC reaction. This was possibly due to absorption and desorption of hydrogen bubbles.

Depth profiling X-ray photoelectron spectroscopy (XPS) was further conducted to understand the interface that might be responsible for the stability improvement. The schematic of XPS depth profile of the electrodes was shown in Figure S12 (Supporting Information). For the unprotected GaAs surface, signals from As—As bonds, lattice As, As_2O_3, and As_2O_5 could all be observed (**Figure 5**a,b). Ga element analysis showed strong Ga_2O_3 signals together with signal from the GaAs lattice (Figure 5c,d). After about 3 cycles of etching, the oxide-related peaks disappeared, suggesting the oxides formed on the unprotected GaAs surface reached almost 6 nm. The full

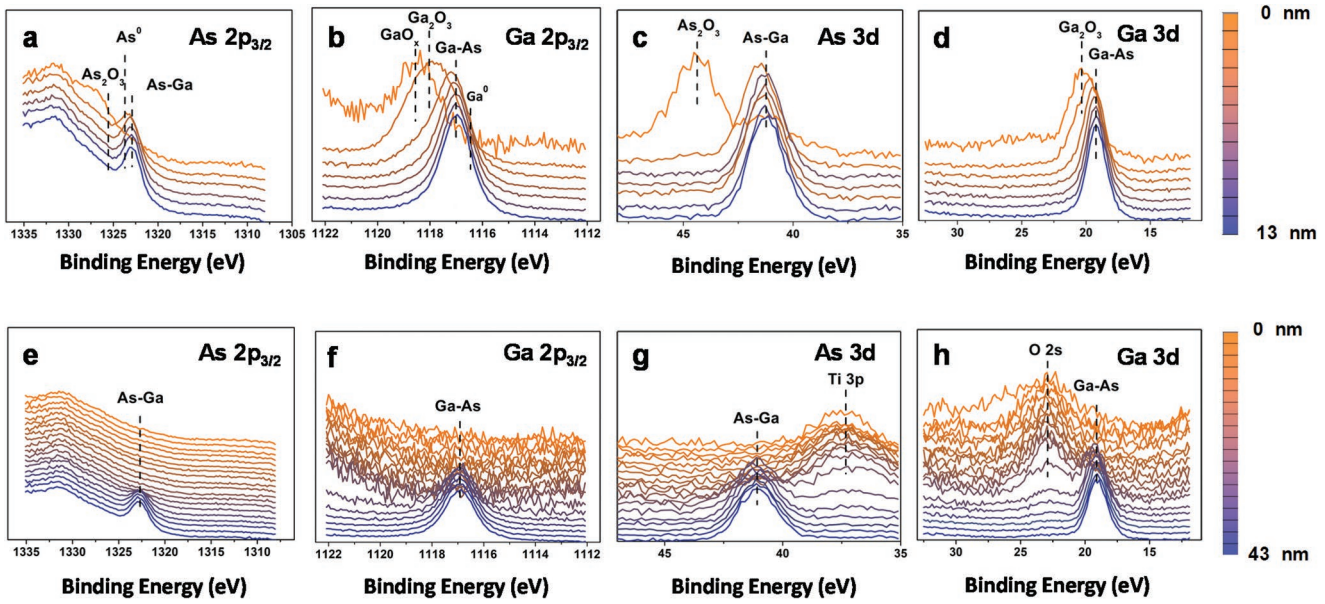

Figure 5. Full depth profile XPS spectra of the unprotected p-GaAs photocathode after photoelectrochemistry a) As $2p_{3/2}$, b) Ga $2p_{3/2}$ and c) As 3d, d) Ga 3d. 300 cycle TiO_2 grown under 300 °C protection layer protected p-GaAs after photoelectrochemistry e) As $2p_{3/2}$ f) Ga $2p_{3/2}$ and g) As 3d, h) Ga 3d.

XPS survey of the unprotected GaAs surface was shown in Figure S14 (Supporting Information). Compared to the unprotected p-GaAs, the TiO_2 protected p-GaAs surface showed negligible oxide formation. After the TiO_2 protection layer was etched away, all the characteristic peaks of As and Ga were associated with the GaAs lattice (Figure 5e–h). No oxide-related As or Ga peaks could be identified. The XPS analysis in Figure 5 confirmed that the unprotected p-GaAs was oxidized by electrolyte during the PEC reaction. The oxides layer on the surface of the p-GaAs could be the main reason for the rapid performance decay as a result of electronic band structure change and poor charge transport property. Coating the surface with optimized TiO_2 could effectively limit the oxidation of GaAs during the PEC reaction, and thus significantly extend the photocathode lifetime.

3. Conclusion

A microdome structured GaAs photocathode was fabricated by metal-assisted chemical etching, which showed enhanced antireflection property. The GaAs surface was protected by various conformal TiO_2 thin films deposited by ALD. PEC tests showed that thicker (26 nm) TiO_2 with a certain degree of crystallization coating via controlled temperature ALD process could provide the best protection against electrolyte corrosion. The J_{ph} of −5.10 mA cm^{-2} remained stable to more than 60 h with only 19.8% reduction. TiO_2 coating further improved the PEC performance by suppressing the surface defects and facilitating charge transfer. The highest saturated J_{ph} reached −12.06 mA cm^{-2} from the patterned GaAs–TiO_2–Pt sample. Depth-resolved XPS analyses revealed that the optimized TiO_2 coating could effectively prevent GaAs from oxidation during the long-term PEC reaction. This work presents a simple and effective strategy to protect GaAs photocathode and to improve its PEC efficiency by precisely tailored crystallinity and accurately controlled thickness ALD coating of TiO_2 thin films. This discovery might eventually open the route toward practical application of III–V compounds for PEC devices.

4. Experimental Section

Fabrication of Patterned p-GaAs Electrode: A 500 µm thick, Zn-doped, single-side-polished, (100)-oriented-GaAs wafer was used as the p-GaAs electrode. The p-type GaAs wafer with a resistivity of $5.17–6.72 \times 10^{17}$ Ω cm was cleaned sequentially in an ultrasonic bath of acetone, ethanol, isopropanol, and distilled (DI) water for 15 min, respectively. 1 M HCl was used to remove the native oxide on the surface p-GaAs. The metal template was formed by lithography. The main processes are shown in Figure S1 (Supporting Information). First, a layer of positive photoresist was spin coated on top of the GaAs. The wafer was heated under 100 °C for 1 min and then exposed to the UV light with a mask covered on surface. After development, a 40 nm layer of Au was evaporated on the GaAs surface. The left photoresist was removed by immersing in an ultrasonic bath of acetone. 0.2370 g $KMnO_4$ was added into 90 mL H_2O and 10 mL H_2SO_4. The solution was used as the etching solution. Water bath was used to keep the temperature between 30 and 35 °C. p-GaAs was immersed in the solution for 5 min. The plane and etched p-GaAs was deposited with Pt particles. The electrode was immersed in the solution containing 1×10^{-3} M H_2PtCl_6 and 0.2 M Na_2SO_4 at the potential of –0.6 V versus Ag/AgCl for 20 min. As shown in Figure S2 (Supporting Information), the Pt particles are uniformly deposited onto the surface of the GaAs. The EDS result shown in Figure S2b (Supporting Information) reveals the existence of GaAs and Pt particles.

ALD Deposition of TiO_2 Thin Film: $TiCl_4$ and H_2O were used as the titanium source and oxygen source, respectfully. Nitrogen was used as the carrier gas with a flow rate of 20 sccm during deposition (base pressure 350 mTorr). One cycle consists of sequence: 0.5 s pulse of H_2O, 60 s N_2 purge, 0.5 s pulse of $TiCl_4$, and 60 s N_2 purge.

TEM Sample Preparation: Cross-sectional TEM samples were prepared via focused ion beam milling. A protective thin film of Pt was deposited

on the surface of the GaAs/TiO_2 sample by ion beam and electronic beam in order to preserve the morphology during milling.

Photoelectrochemical Measurement: The photoelectrochemical measurement was conducted by using an Autolab PGSTAT302N station. A three-electrode system was implemented for PEC measurements. p-GaAs photocathode, a Pt wire, and a Ag/AgCl electrode are the working, counter, and reference electrodes, respectively. 0.1 M potassium phosphate electrolyte solution (pH 7) was used as the electrolyte. Working electrode was illuminated by a 150 W xenon lamp coupled with an AM 1.5 global filter with a light intensity of 100 mW cm^{-2}. Impedance data were gathered using a 100 mV amplitude perturbation in the frequency range between 10 000 to 1 Hz at an applied voltage of –1.2 V versus Ag/AgCl.

Characterization: SEM and EDS observations were performed on a Zeiss LEO 1530 field-emission microscope. TEM observation was performed on a Tecnai G2 F20 U-TWIN microscope. Focused ion beam cutting was carried out by means of a FIB Nova 200 NanoLab. XPS depth profile was acquired using a Thermo Scientific K-alpha XPS instrument, ion beam was rastered over a square area of the sample. After the etch cycle, the ion beam is blanked and another set of spectra is recorded. The reflectance spectra were recorded using a Jasco V-570 UV–vis spectrophotometer with an integrating sphere.

FDTD Simulation: The planar and patterned GaAs electrodes were optically simulated using the Finite Difference Time Domain. The software was FDTD Solutions 8.6 from Lumerical Solutions. The wavelength dependence of the absorption profiles of the GaAs can be obtained from the refractive index of the FDTD material library which is included in the FDTD software. The refractive index data of the corresponding material can be directly selected during the simulation process. As shown in Figure S3 (Supporting Information), two FDTD simulation models of planar GaAs and patterned GaAs were designed. The incident plane wave was illuminated from the up side with a simulation time of 1000 fs. The wavelengths of the plane wave were chosen as 580 and 850 nm, respectively.

Supporting Information

Supporting Information is available from the Wiley Online Library or from the author.

Acknowledgements

S.Y.C. and Z.K. contributed equally to this work. This work was supported by the National Natural Science Foundation of China (51527802, 51602020, 51722203, 51672026, 51772024, 51702014), the Overseas Expertise Introduction Projects for Discipline Innovation (No. B14003), the Beijing Natural Science Foundation (Z180011), the National Key Research and Development Program of China (2016YFA0202701, 2018YFA0703503).

Conflict of Interest

The authors declare no conflict of interest.

Keywords

atomic layer deposition, GaAs, photocathode stability, photoelectrochemical water splitting, TiO_2 coating

Received: September 11, 2019
Revised: November 25, 2019
Published online: January 31, 2020

[1] a) M. M. May, H.-J. Lewerenz, D. Lackner, F. Dimroth, T. Hannappel, *Nat. Commun.* **2015**, *6*, 8286; b) O. Khaselev, J. A. Turner, *Science* **1998**, *280*, 425; c) D. Bae, B. Seger, P. C. K. Vesborg, O. Hansen, I. Chorkendorff, *Chem. Soc. Rev.* **2017**, *46*, 1933.

[2] C. Jiang, S. J. A. Moniz, A. Wang, T. Zhang, J. Tang, *Chem. Soc. Rev.* **2017**, *46*, 4645.

[3] a) S. Chen, L.-W. Wang, *Chem. Mater.* **2012**, *24*, 3659; b) K. Walczak, Y. Chen, C. Karp, J. W. Beeman, M. Shaner, J. Spurgeon, I. D. Sharp, X. Amashukeli, W. West, J. Jin, N. S. Lewis, C. Xiang, *ChemSusChem* **2015**, *8*, 544; c) O. Savadogo, *Sol. Energy Mater. Sol. Cells* **1998**, *52*, 361; d) M. Pourbaix, *Atlas of Electrochemical Equilibria*, National Association of Corrosion Engineers, Houston, TX **1974**.

[4] a) M. V. Lebedev, W. Calvet, T. Mayer, W. Jaegermann, *J. Phys. Chem. C* **2014**, *118*, 12774; b) J. L. Young, K. X. Steirer, M. J. Dzara, J. A. Turner, T. G. Deutsch, *J. Mater. Chem. A* **2016**, *4*, 2831.

[5] K. Sun, F. H. Saadi, M. F. Lichterman, W. G. Hale, H.-P. Wang, X. Zhou, N. T. Plymale, S. T. Omelchenko, J.-H. He, K. M. Papadantonakis, B. S. Brunschwig, N. S. Lewis, *Proc. Natl. Acad. Sci. USA* **2015**, *112*, 3612.

[6] F. Yang, A. C. Nielander, R. L. Grimm, N. S. Lewis, *J. Phys. Chem. C* **2016**, *120*, 6989.

[7] B. A. Pinaud, J. D. Benck, L. C. Seitz, A. J. Forman, Z. Chen, T. G. Deutsch, B. D. James, K. N. Baum, G. N. Baum, S. Ardo, H. Wang, E. Miller, T. F. Jaramillo, *Energy Environ. Sci.* **2013**, *6*, 1983.

[8] a) L. Kornblum, D. P. Fenning, J. Faucher, J. Hwang, A. Boni, M. G. Han, M. D. Morales-Acosta, Y. Zhu, E. I. Altman, M. L. Lee, C. H. Ahn, F. J. Walker, Y. Shao-Horn, *Energy Environ. Sci.* **2017**, *10*, 377; b) D. Kang, J. L. Young, H. Lim, W. E. Klein, H. Chen, Y. Xi, B. Gai, T. G. Deutsch, J. Yoon, *Nat. Energy* **2017**, *2*, 17043; c) L. E. Garner, K. X. Steirer, J. L. Young, N. C. Anderson, E. M. Miller, J. S. Tinkham, T. G. Deutsch, A. Sellinger, J. A. Turner, N. R. Neale, *ChemSusChem* **2017**, *10*, 767.

[9] S. Hu, M. R. Shaner, J. A. Beardslee, M. Lichterman, B. S. Brunschwig, N. S. Lewis, *Science* **2014**, *344*, 1005.

[10] a) T. Wang, Z. Luo, C. Li, J. Gong, *Chem. Soc. Rev.* **2014**, *43*, 7469; b) R. Liu, Z. Zheng, J. Spurgeon, X. Yang, *Energy Environ. Sci.* **2014**, *7*, 2504; c) J. Zheng, Y. Lyu, R. Wang, C. Xie, H. Zhou, S. P. Jiang, S. Wang, *Nat. Commun.* **2018**, *9*, 3572; d) S. Hu, N. S. Lewis, J. W. Ager, J. Yang, J. R. McKone, N. C. Strandwitz, *J. Phys. Chem. C* **2015**, *119*, 24201; e) Y. He, T. Hamann, D. Wang, *Chem. Soc. Rev.* **2019**, *48*, 2182.

[11] Y. Yu, Z. Zhang, X. Yin, A. Kvit, Q. Liao, Z. Kang, X. Yan, Y. Zhang, X. Wang, *Nat. Energy* **2017**, *2*, 17045.

[12] Y. Yu, C. Sun, X. Yin, J. Li, S. Cao, C. Zhang, P. M. Voyles, X. Wang, *Nano Lett.* **2018**, *18*, 5335.

[13] a) M. DeJarld, J. C. Shin, W. Chern, D. Chanda, K. Balasundaram, J. A. Rogers, X. Li, *Nano Lett.* **2011**, *11*, 5259; b) Y. Song, J. Oh, *J. Mater. Chem. A* **2014**, *2*, 20481.

[14] a) R. Yu, K.-L. Ching, Q. Lin, S.-F. Leung, D. Arcrossito, Z. Fan, *ACS Nano* **2011**, *5*, 9291; b) S.-F. Leung, M. Yu, Q. Lin, K. Kwon, K.-L. Ching, L. Gu, K. Yu, Z. Fan, *Nano Lett.* **2012**, *12*, 3682; c) Z. Fan, H. Razavi, J.-w. Do, A. Moriwaki, O. Ergen, Y.-L. Chueh, P. W. Leu, J. C. Ho, T. Takahashi, L. A. Reichertz, S. Neale, K. Yu, M. Wu, J. W. Ager, A. Javey, *Nat. Mater.* **2009**, *8*, 648.

[15] S. Dueñas, H. Castán, H. García, E. S. Andrés, M. Toledano-Luque, I. Mártil, G. González-Díaz, K. Kukli, T. Uustare, J. Aarik, *Semicond. Sci. Technol.* **2005**, *20*, 1044.

[16] H. Gerischer, N. Müller, O. Haas, *J. Electroanal. Chem. Interfacial Electrochem.* **1981**, *119*, 41.

[17] J. Qiu, H. Hajibabaei, M. R. Nellist, F. A. L. Laskowski, S. Z. Oener, T. W. Hamann, S. W. Boettcher, *ACS Energy Lett.* **2018**, *3*, 961.

[18] A. Ramos-Ruiz, J. A. Field, W. Sun, R. Sierra-Alvarez, *Waste Manage.* **2018**, *77*, 1.

